

Appendix

Cost-effectiveness of the alternative uses of polyvalent meningococcal vaccines in Niger: an agent-based transmission modeling study

S1 Additional Details on the Agent-Based Simulation Model

Agents in our agent-based model (ABM) for meningococcal epidemics represent individual population members. An agent's attributes include id, age (in weeks: 0, 1, ..., 52000, where 52000 is the theoretical maximum), age group (<1, 1-4, 5-9, 10-14, 15-19, 20-24, 25-29, 30-34, 35-39, 40-44, 45-49, 50-54, 55-59, 60-64, 65-69, 70-74, 75-79, 80-84, 85-89, 90-94, 95-99, 100+ years old), district, current health state (Susceptible, Carrier, Meningitis, Immune), and various *timer* variables which track the time until the next scheduled event (e.g. death or infection) will occur. An agent's vaccination status is also recorded: vaccinated or not, and if vaccinated, then the vaccine name (*MenAfriVac*TM, PMP, or PMC) and the vaccination program code (routine, reactive, or preventive).

A simplified class diagram of the model architecture in the ABM is shown in Figure S1. The Model class¹ is used to specify the simulation's seed, the random data generator object, the current time step counter, the districts, and the vaccination campaign (optional). It also contains all AgeGroup classes, each of which in turn contains a list of Agent classes (for agents which fall under that age group). Each Agent class contains agent's attributes including id, age (in weeks), district, current health state, vaccination status, etc. Each District class contains its dynamic population data (e.g. total number of infected people and total number of people) and dynamic transmission data (e.g. force of infection and mean time of infection), which are re-calculated during each week.

¹ Technically, we mean "an instance of a class" when we refer to "a class".

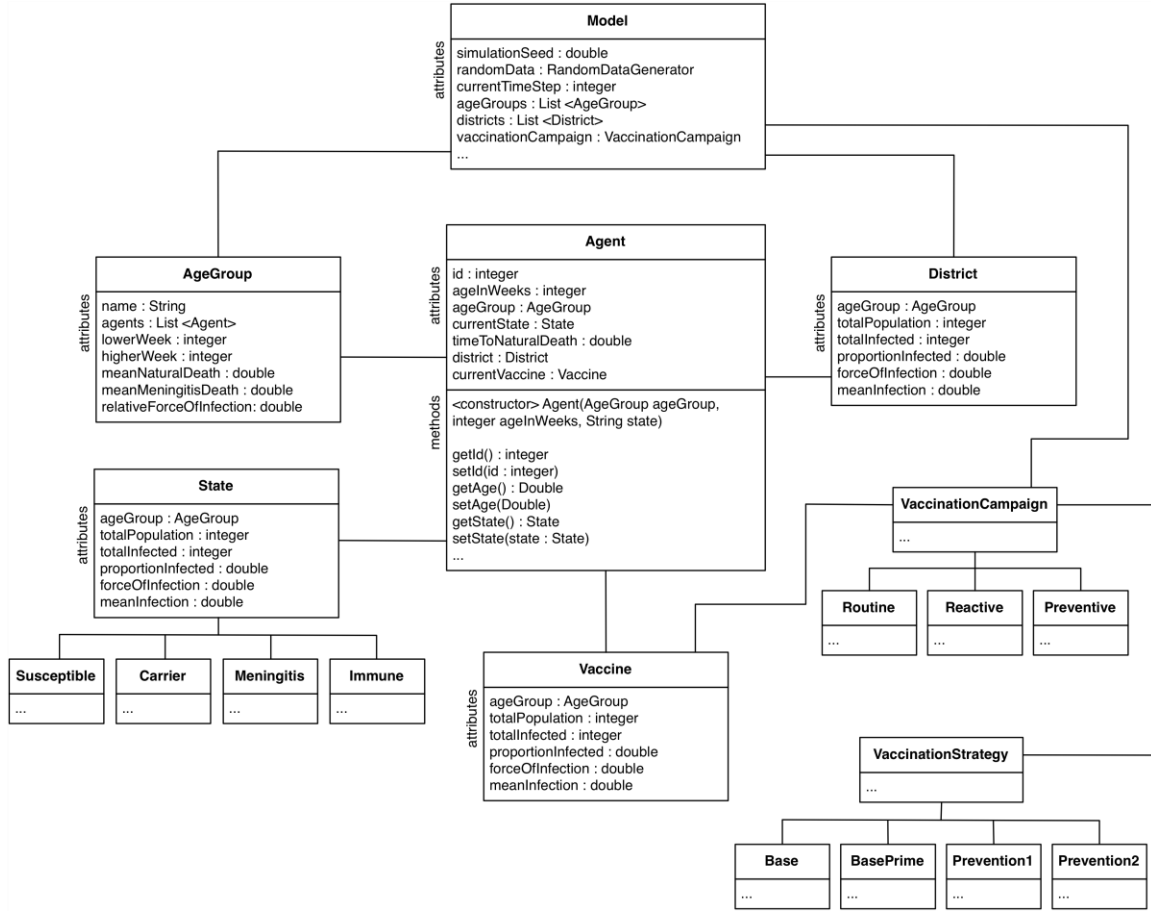


Figure S1: A simplified class diagram of the model architecture in the ABM. For simplicity, attributes and methods of most classes are omitted. We use the terms model and simulation interchangeably.

Random Number Generators

Our ABM utilizes the Apache Commons Math random package [63] to generate stochastic distributions and epidemic trajectories. To obtain a specific trajectory, we first specify the seed of the simulation's the random number generator (RNG) object and the simulator will then use the RNG object to generate a unique stream of random numbers which will be used to both draw a sample for epidemic parameters and to generate the simulated trajectory. This approach will enable us to regenerate any desired trajectory by providing the corresponding RNG seeds. Since the calibration procedure is sensitive to the simulation's seed, which in turn affects the RNG object, we use a second RNG object for the vaccination scenarios to generate a separate stream of random numbers.

Model Initialization and Execution

The model is initialized with populations of Niger districts in year 2002. For all districts, initial populations are created, and their ages are set using random samples from the distributions of Niger's age-structure (stratified into the 22 age groups, see Table S1). Newly born individuals are assigned to a district randomly according to probability weights proportional to the district populations in 2016 [64]. The simulation time-step is set to 1 week.

Each simulation includes a 1-year warm-up period, and is run for either 13.5 or 28 years for purposes of calibration and evaluating vaccination scenarios, respectively.

S2 Niger: Study Area and Demography

The estimated population of Niger is 18,638,600 (July 2016 est.) with 44.8 births/1,000 population in 2016 [64]. Niger is divided into eight administrative regions and 44 districts. The centroid and population of each district are shown in Figure S2, and the straight-line distances (in miles, calculated using the Haversine formula [65]) between districts are shown in Figure S3. The 2014 population data, obtained from the Niger Ministry of Health [66], are discounted at an annual growth rate of 3.22% (2016 est.) to 2002 [64]. The district-level spatial disaggregation enables us to model reactive vaccination campaigns that are triggered for each district once it passes the WHO epidemic threshold of 10 per 100,000 per week [4].

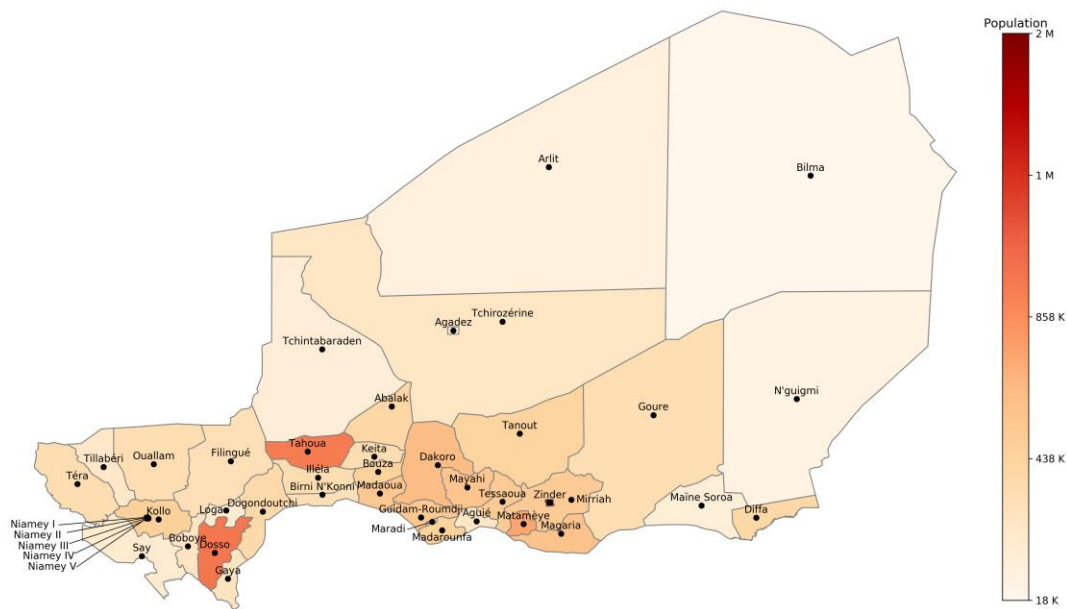


Figure S2: Study area depicting the centroids and populations of 44 districts of Niger. The 2002 population data, obtained from the Niger Ministry of Health, are discounted at an annual growth rate of 3.22% (2016 est.) [64] from 2014.

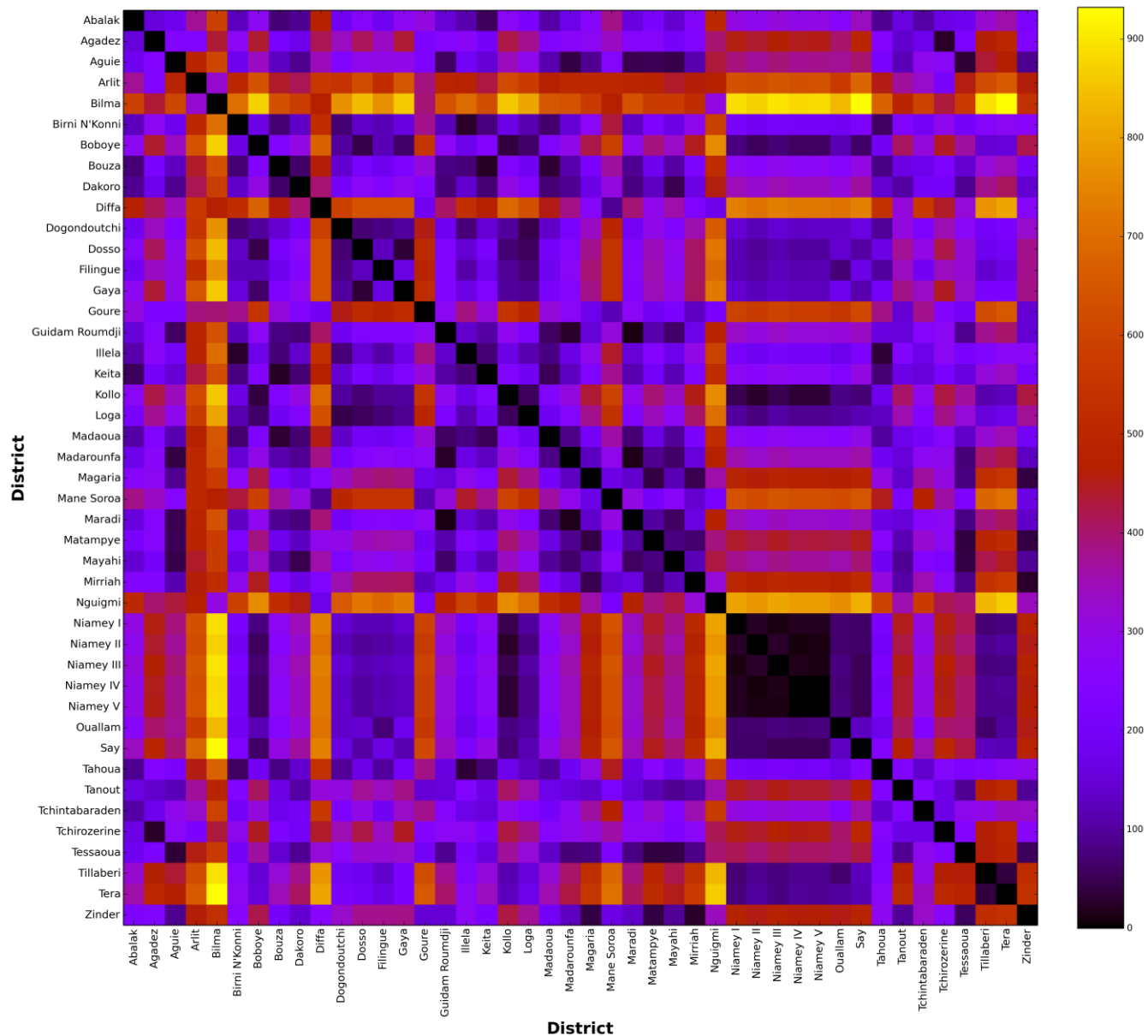


Figure S3: Distance matrix for all districts of Niger. Distances (in miles) between districts are calculated using the Haversine formula [65] and the coordinates of districts by Python.

Our model includes 22 age groups (<1, 1-4, 5-9, 10-14, 15-19, 20-24, 25-29, 30-34, 35-39, 40-44, 45-49, 50-54, 55-59, 60-64, 65-69, 70-74, 75-79, 80-84, 85-89, 90-94, 95-99, 100+ years old) to allow for age-specific mixing patterns and to permit age-specific targeting of vaccinations. We use Niger's population life tables [67] to estimate the proportion of the population into these age groups. The age-stratified mortality rates are also informed by population data (Table S1) [64].

Table S1: Niger demography [65, 67].

Index	Age Group	Age Distribution (%)	Annual Mortality Rate
1	<1	0.02789	0.0595
2	1-4	0.16732	0.0105
3	5-9	0.16509	0.002
4	10-14	0.13274	0.001
5	15-19	0.10262	0.002
6	20-24	0.07697	0.003
7	25-29	0.0647	0.003
8	30-34	0.05466	0.003
9	35-39	0.04573	0.004
10	40-44	0.03904	0.005
11	45-49	0.03123	0.0065
12	50-54	0.02454	0.0095
13	55-59	0.02008	0.0135
14	60-64	0.0145	0.021
15	65-69	0.01115	0.034
16	70-74	0.00892	0.0585
17	75-79	0.00558	0.1005
18	80-84	0.00279	0.169
19	85-89	0.00112	0.27
20	90-94	0.00112	0.4005
21	95-99	0.00112	0.517
22	100+	0.00112	0.647

S3 Natural History and Transmission Dynamics

The prior distributions of natural history, transmission dynamics, and seasonality parameters are described in T9-12. Adopting the notation of [33], we calculate the force of infection at time t for susceptible members in age group i of district k as:

$$F_{k,i}(t) = \beta_{k,i}(t) \sum_{(k',i')} \lambda_{(k,i) \leftarrow (k',i')} \frac{I_{(k',i')}(t)}{N_{(k',i')}(t)} \quad (1)$$

where $\beta_{k,i}(t)$ is the transmission parameter for district k and age group i , and $N_{(k,i)}(t)$ and $I_{(k,i)}(t)$ denotes, respectively, the population size of district k and the number of infectious members in district k that belong to age group i . We let $\beta_{k,i}(t) = d_k \beta_i(t)$, where d_k is the proportion of *N. meningitidis* cases in Niger between 2002-2016 (obtained from the anonymized individual-level dataset provided by the Ministry of Health, Niger) that was observed in district k . As demonstrated by previous studies, regional climate variability impacts meningitis activities with epidemics occurring in the dry season and receding with the onset of the rainy season [68, 69]. To capture the effect of seasonal changes on meningitis epidemics, we allow the transmission parameter $\beta_i(t)$ in Eq. (2) to vary over time according to:

$$\beta_i(t) = \begin{cases} \gamma_{i,1}(a_0 + a_{1,q} \cos 2\pi(t + a_2)), & \text{if } q \leq t \leq (2q + 1)/2, \\ \gamma_{i,1}a_0, & \text{otherwise.} \end{cases} \quad (2)$$

In Eq. (2), the integer q denotes the year number of time t , and the condition $q \leq t \leq (2q + 1)/2$ implies that this seasonality effect is present only during the first half of each year. This is consistent with historical data that show meningitis epidemics occur in dry seasons and disappear with the onset of rainy seasons that last approximately 4 months from May/June to September (Figure 2). Parameter s_0 in Eq. (2) is the baseline transmissibility which is not influenced by the seasonality effect, and the parameter $s_{1,q}$ represents the maximum magnitude of seasonality effect during year q . To account for between-year variation in transmission due to other external causes, we allow $s_{1,q}$ to be randomly drawn from a uniform probability distribution. We found that this approach, which has been previously employed in other models [33, 39], is important for the generation of epidemics with the ranges of magnitudes observed in historical data (Figure 2). The phase parameter s_2 is also included to provide additional flexibility in the modeling of the seasonality effect. We chose $s_0 = 0$ and $s_2 = -0.25$ which result in a seasonality effect that gradually increases from January, peaks around May and diminishes by September.

Meningitis incidence and carriage prevalence vary across age groups and districts [70-73]. Hence, we also allow the transmission parameter to be age- and district- dependent: in Eq. (2), parameter $\gamma_{i,1}$ in $\beta_i(t)$ denotes the relative force of infection in age group i with respect age group (" < 1 ") in the absence of seasonality ($\gamma_{1,1} = 1$), and in Eq. (1), parameter d_k in $\beta_{k,i}(t)$ denotes the district-level transmission coefficient for district k .

Individuals who get infected move to the health state Carrier and are assumed to be protected against superinfection. While in this health state, an agent who belong to age group i may progress to the invasive disease at the rate $m_i(t_{\text{Inf}}) = a_i e^{-t_{\text{Inf}}}$, where $a_i > 0$ is determined through calibration, and t_{Inf} is the time elapsed since infection. We assume that meningitis lasts for a week and its mortality is 10% ($\kappa = 0.1$) (see Table S3).

Individuals transition to the Immune state upon losing their carriage status or recovering from meningitis. Based on how they acquired their immunity (losing carriage or recovering from meningitis), the duration of stay in this state is set as follows. If an individual did not have meningitis, the duration is sampled from a probability distribution that is characterized through calibration (Table S3). Otherwise (i.e. if it had meningitis), it is sampled from the same distribution and multiplied by a ratio (of time until losing immunity from disease to time until losing immunity from carriage), which is sampled from a ratio distribution of that is characterized through calibration (Table S3).

S4 A Gravity Model to Estimate Age-Specific Contact Rates Within and Between Districts

For Niger, population-based survey data of epidemiologically relevant social contact patterns (such as the POLYMOD dataset [74] which provides social contact matrices for eight different European countries) do not

exist. Hence, to model the contact patterns between individuals in different age groups residing in different districts of Niger, we use age-structured contact matrices projected from a recent Bayesian hierarchical study [75] which described the age-specific mixing pattern of individuals in 152 countries, including Niger. The contact matrix $[\bar{\lambda}_{i,i'}]$, extended from 15 to 22 age groups for the ABM, is shown in Figure S4. Adopting the notation of [33], we let $d_{k,k'}$ denote the distance between districts k and k' , and n_k denote the population of district k . We use $\lambda_{(k,j) \leftarrow (k',j')}$ to denote the daily rate at which an average individual in age group i of district k contacts with individuals in age group i' of district k' . Assuming that during each day an individual in age group i contacts on average with $\bar{\lambda}_{i,i'}$ individuals in age group i' , we estimate $\lambda_{(k,j) \leftarrow (k',j')}$ by:

$$\lambda_{(k,j) \leftarrow (k',j')} = \bar{\lambda}_{i,i'} \frac{f(d_{k,k'}) \frac{n_k}{n_{k'}}}{\sum_{k'} f(d_{k,k'}) \frac{n_k}{n_{k'}}}, \quad (3)$$

where f is a monotonically decreasing function. Here, we use $f(d) = e^{-0.003d}$, informed by a previous study [33]. Eq. (3) holds the assumption that the number of contacts between two districts (k, k') is proportional to the multiple of some distance weight function (i.e. $f(d_{k,k'})$) and the relative size of the districts (i.e. $\frac{n_k}{n_{k'}}$). We employ the Haversine formula [65] and the coordinates of districts to approximate distance between districts (i.e. $d_{k,k'}$).

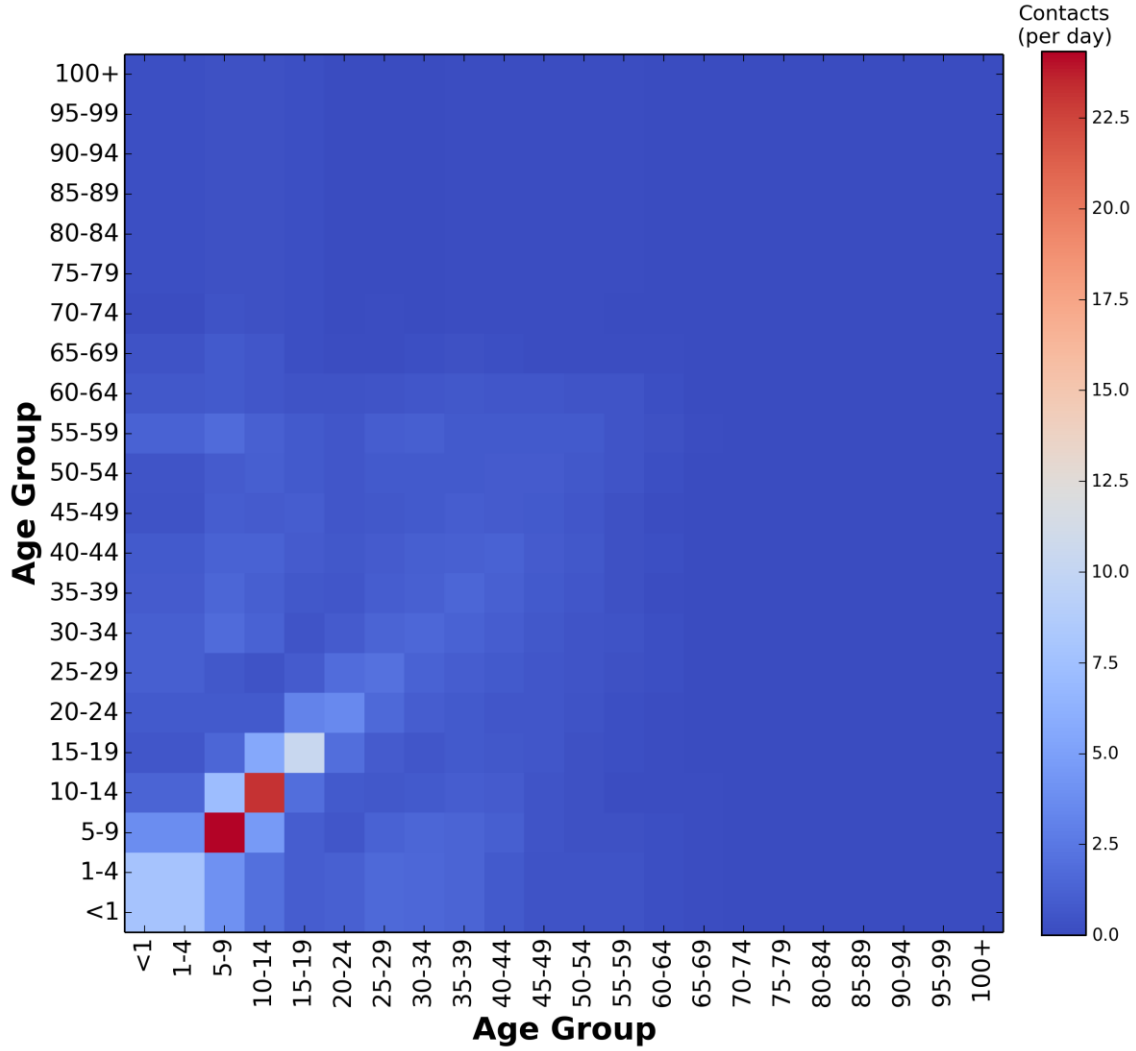


Figure S4: Average daily number of contacts among different age groups calculated from a recent Bayesian hierarchical study which described the age-specific mixing pattern of individuals for Niger [75]. The original contact matrix is extended from 15 to 22 age groups for the ABM.

S5 Data Sources to Inform Calibration Targets

We use an anonymized individual-level dataset of reported meningitis cases in Niger between 2002 to mid-2015 (provided by the Ministry of Health, Niger) to prepare our data sources against which we calibrate the model (i.e. the weekly number of *Neisseria meningitis* cases, within Niger districts, associated to A and non-A serogroups, and the age-distribution of cases). The dataset contains sample date, district, age, and the conclusion made for 29,349 clinical cases. Conclusions could be negative, *N. meningitidis* serogroup A, C, W and X, *Streptococcus pneumoniae* and *Haemophilus influenzae* type b, and is made using different methods such as polymerase chain reaction (PCR), microorganism conclusion, aspect macro LCR, resultat gram, Latex test, and culture. We applied a simple extrapolation method to determine the value of missing date and age as described below).

Missing dates

For patients where the date of final diagnosis is missing, we first look at the sample date column. If it is missing, we successively look at the date of reception, then the date of the first appearance of disease, and then the date of the patient's consultation – whichever is present and comes first in the order. The ranges of dates for all 29,349 records are 2/12/02 - 6/29/15.

Missing patient's age

A total of 3721 records have both age in years and in months missing. We use empirical distributions of the age group-distribution of each epidemic season to assign an age group to cases with missing age. This is performed as follows. From the original 29,349 records, we aggregate the records by year, and calculate the age-distribution of cases for each year. We then used these empirical distributions to determine the age of patients with missing values. The 3721 patient records with missing age values are classified into the five age groups as 175 (“<1”), 1073 (“1–4”), 1812 (“5–14”), 458 (“15–29”), and 203 (“30+”).

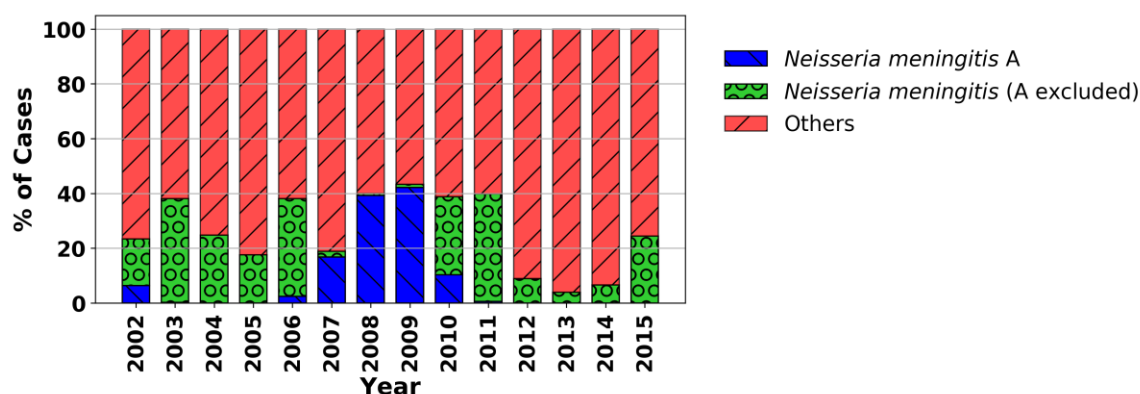


Figure S5: Percentage of confirmed meningitis cases that are associated to *N. meningitidis* serogroup A, *N. meningitidis* non-A serogroups (including C, W, and X), and other pathogens (including *Streptococcus pneumoniae* and *Haemophilus influenzae* type b) in Niger from 2002 to mid-2015.

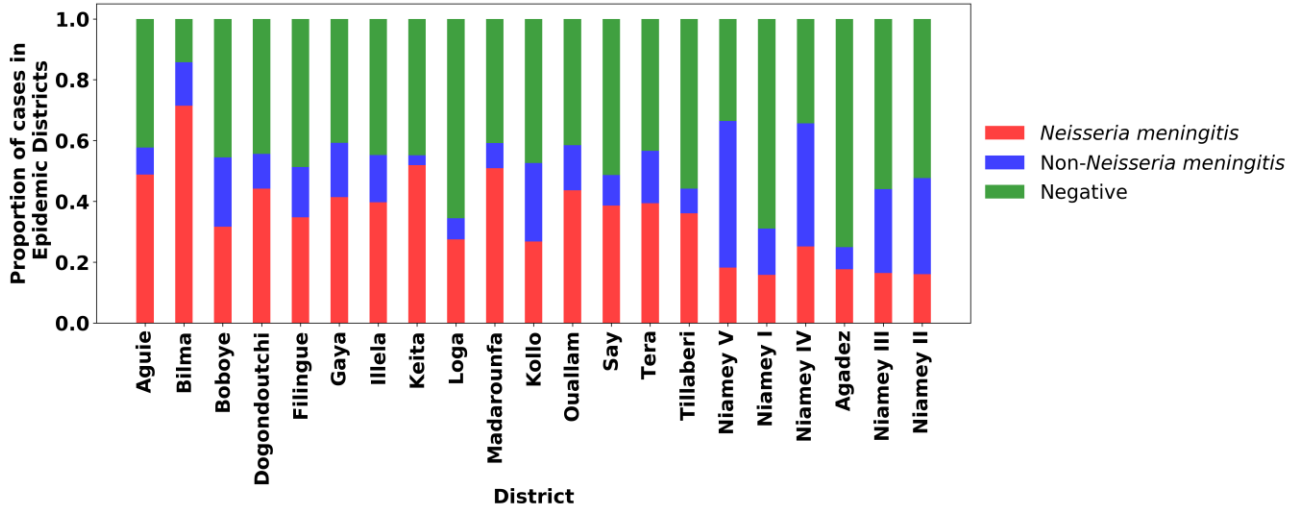


Figure S6: Percentage of reported meningitis cases in epidemic districts of Niger from 2002 to mid-2015 with “*Neisseria meningitidis*”, “Non-*Neisseria meningitidis*,” or “Negative” as final conclusion. This figure demonstrates the potential level of underreporting of meningococcal cases in the dataset used for calibrating our transmission model as most meningitis cases (>79%) in epidemic years 2006-8 were caused by *N. meningitidis* [18].

Estimating Age-Specific Carriage Prevalence

For the complete strain replacement scenario, we obtained the estimates for age-specific meningococcal carriage prevalence ($CP_{CSR,i}$ for age group $i \in \{1, 2, \dots\}$) from a carriage survey study conducted in the African meningitis belt (Table S2) [19]. For the no strain replacement scenario, we estimated the age-specific carriage prevalence using the following approach. For age group i , we define:

$$\text{ratio}_i = \frac{\text{number of cases due to N. serogroup A in age group } i}{\text{number of cases due to all N. serogroups in age group } i}$$

The carriage prevalence for age group i for the no strain replacement scenario is then estimated as (Table S2):

$$CP_{NSR,i} = \text{ratio}_i \times CP_{CSR,i}.$$

Table S2: Age-specific cases and carriage prevalence used for calibrating the model under two strain-replacement scenarios

Age Group	Complete Strain Replacement		No Strain Replacement	
	Cases	Carriage Prevalence (%)	Cases	Carriage Prevalence (%)
<1	371	1.8	296	1.44
1-4	2388	2.6	1689	1.84
5-14	5087	4.9	3208	3.09
15-29	1159	3.6	817	2.54
30+	299	2.6	229	1.99

S6 Estimating Clinical Meningitis Cases

Reactive vaccination campaigns are launched in districts where the weekly number of clinical meningitis cases (which include cases due to all *N. meningitidis* serogroups, and other cases due to e.g. *H. influenzae* types b and non-b, *S. pneumonia*) passes the WHO epidemic threshold of 10 per 100,000 per week [4]. We therefore use the following approach to construct the clinical meningitis time-series based on the weekly meningococcal incidence produced by our model. These constructed district-level meningitis time-series are then used to decide if reactive campaigns should be triggered throughout a simulation run.

Let

- $y_{\text{CSR}}(t, k)$ denote the number of meningococcal cases per 100,000 population, caused by all *N. meningitidis* serogroups, observed in district k over week t ,
- $y_{\text{NSR}}(t, k)$ denote the number of meningococcal cases per 100,000 population, caused by all *N. meningitidis* serogroups except serogroup A, observed in district k over week t , and
- $y_{\text{Others}}(t, k)$ denote the number of clinical meningitis cases per 100,000 population that are confirmed negative or associated to non- *N. meningitidis* serogroups (e.g. *H. influenzae* types b and non-b, *S. pneumonia*), observed in district k over week t .

Our goal is to find a regression model $M(\cdot)$ that returns an estimate for $y_{\text{Others}}(t, k)$ if $\hat{y}_{\text{CSR}}(t, k)$ and $\hat{y}_{\text{NSR}}(t, k)$ are what our simulation model produces for the number of meningococcal cases per 100,000 population in district k during week t , for complete strain replacement and no strain replacement scenarios. Fitting a 3rd degree polynomial (least squares polynomial fit) function of week t and the number of meningococcal cases ($y_{\text{CSR}}(t, k)$ or $y_{\text{NSR}}(t, k)$ depending on the strain replacement scenario) to $y_{\text{Others}}(t, k)$, we characterized the regression model $M(\cdot)$ for the complete strain replacement scenario as:

$$\begin{aligned} \check{y}_{\text{Others,CSR}}(t, k) = & -5.33357444 \times 10^{-4} \times \hat{y}_{\text{CSR}}(t, k)^3 + 8.96344860 \times 10^{-2} \times \hat{y}_{\text{CSR}}(t, k)^2 \\ & + 1.08069657 \times \hat{y}_{\text{CSR}}(t, k) + 7.85514925 \times 10^{-2}, \end{aligned}$$

and for the no strain replacement scenario as:

$$\begin{aligned} \check{y}_{\text{Others,NSR}}(t, k) = & -5.96859698 \times 10^{-4} \times \hat{y}_{\text{NSR}}(t, k)^3 + 8.52547129 \times 10^{-2} \times \hat{y}_{\text{NSR}}(t, k)^2 \\ & + 1.41036290 \times \hat{y}_{\text{NSR}}(t, k) + 9.57915532 \times 10^{-2}. \end{aligned}$$

Figure S7 shows that these regression models fit the outcomes (i.e. $y_{\text{Others}}(t, k)$) properly. Using these regression models, we can now determine the number of clinical meningitis cases per 100,000 population in district k over the simulation week t by:

$$\check{y}_{\text{Others,CSR}}(t, k) + \check{y}_{\text{CSR}}(t, k),$$

for the complete strain replacement scenario and

$$\check{y}_{\text{Others,NSR}}(t, k) + \check{y}_{\text{NSR}}(t, k),$$

for the no strain replacement scenario. A reactive campaign is launched in district k if the clinical incidence passes the WHO epidemic threshold.

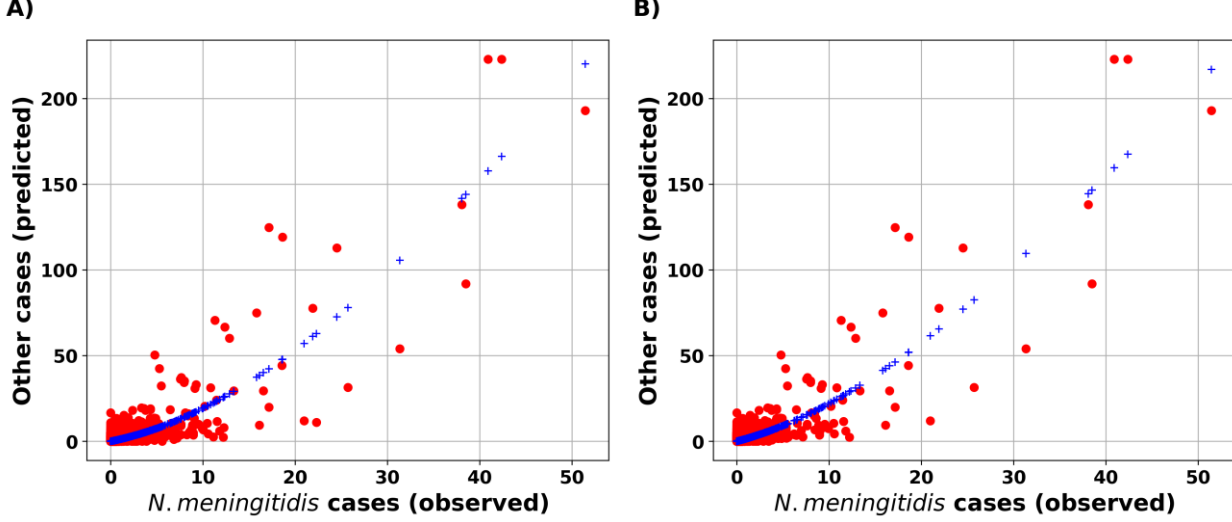


Figure S7: Estimating “other” (Non-*N. meningitidis* and negative) cases using non-linear regression. A) Complete strain replacement scenario. B) No strain replacement scenario.

S7 Model Calibration

Our calibration approach is adopted from [33] and extended for the ABM developed here. For each strain replacement scenario, we measure the fit of a simulated trajectory with respect to the average and periodicity in the weekly number of meningococcal cases, age-distribution of meningococcal cases, and average prevalence of meningococcal carriage in age groups. To build a set of trajectories to evaluate the performance of vaccination strategies in Table 3, we first simulate 100,000 epidemic trajectories (for each scenario), each of which uses parameter values that are randomly drawn from the prior probability distributions listed in Table S3-Table S5. These prior distributions are mainly informed by estimates extracted from existing scientific literature. When such estimates are not available, we identified prior distributions by experimenting with the model (“hand-fitting”) to ensure the model can produce simulated trajectories that are consistent with past observations. Then, we eliminate trajectories that eventually “die-out” (e.g., have zero meningitis cases in one or more years of the last 5 years), and select the best-fitting 200 epidemic trajectories for evaluating control policies.

We use the approach described below to approximate the likelihood of observations given a simulated trajectory. In this approach, to obtain one simulated epidemic trajectory, we first specify the seed of the simulation’s random number generator (RNG) object. The simulator will then use the RNG object to generate a unique stream of random numbers which will be used to both draw a sample for epidemic parameters and to generate one simulated trajectory. This approach will enable us to regenerate any desired trajectory by providing the corresponding RNG seeds. In the following, we use $i \in \{1, 2, \dots, 5\}$ to denote the age groups $\{<1, 1-4, 5-14, 15-29, 30+\}$ and $k \in$

$\{1, 2, \dots, 44\}$ to denote districts of Niger. Our chosen pseudolikelihood function consists of 4 components as explained below:

Component 1. Likelihood of age-distribution of cases

Let $\hat{\tau}_i$ denote the number of meningococcal cases in age group $i \in \{1, 2, \dots, 5\}$ observed between 2002 and mid-2015. For the scenario with strain replacement, $(\hat{\tau}_1, \hat{\tau}_2, \hat{\tau}_3, \hat{\tau}_4, \hat{\tau}_5) = (371, 2388, 5087, 1159, 299)$, and for the scenario without strain replacement, $(\hat{\tau}_1, \hat{\tau}_2, \hat{\tau}_3, \hat{\tau}_4, \hat{\tau}_5) = (296, 1689, 3208, 817, 229)$ (see Table S2). We assume that $(\hat{\tau}_1, \hat{\tau}_2, \hat{\tau}_3, \hat{\tau}_4, \hat{\tau}_5)$ follows a multinomial distribution with $\sum_{i=1}^5 \hat{\tau}_i = 9304$ or 6239 trials (for with and without strain-replacement scenarios) and success probabilities $(\tau_{z,1}, \tau_{z,2}, \tau_{z,3}, \tau_{z,4}, \tau_{z,5})$, where $\tau_{z,i}$ is the percentage of meningococcal cases that belong to age group i in a simulated trajectory for which RNG seed z is used.

Component 2. Likelihood of average carriage prevalence

Let \hat{S}_i and \hat{s}_i be, respectively, number of participants and number of confirmed as meningococcal in age group $i \in \{1, 2, \dots, 5\}$ during the 2009-2012 meningococcal carriage survey study in the African meningitis belt [73]. We assume that \hat{s}_i follows a binomial distribution with \hat{S}_i trials and success probability $\rho_{z,i}$, where $\rho_{z,i}$ is the average prevalence of meningococcal carriage in age group i in a simulated trajectory for which RNG seed z is used, and $(\hat{S}_1, \hat{S}_2, \hat{S}_3, \hat{S}_4, \hat{S}_5) = (2199, 8839, 13121, 12425, 11906)$ [73]. For the scenario with strain replacement, we set $(\hat{s}_1, \hat{s}_2, \hat{s}_3, \hat{s}_4, \hat{s}_5) = (41, 228, 655, 450, 313)$, and for the scenario without strain replacement we set $(\hat{s}_1, \hat{s}_2, \hat{s}_3, \hat{s}_4, \hat{s}_5) = (32, 163, 405, 316, 237)$, which is calculated by multiplying the estimated carriage prevalence under no strain replacement scenario (column 5 in Table S2) by the number of survey participants in each age group, i.e. $(\hat{S}_1, \hat{S}_2, \hat{S}_3, \hat{S}_4, \hat{S}_5) = (2199, 8839, 13121, 12425, 11906)$.

Component 3. Likelihood of average weekly meningitis incidence

Let \hat{y}_t denote the meningitis cases observed during week $t \in \{1, 2, \dots, T\}$, where $T = 702$ denotes the total number of weeks in 2002 to mid-2015. We assume that the mean of observed weekly meningitis cases, i.e. $\mu_{\hat{y}} = \sum_{t=1}^T \hat{y}_t / T$, follows a normal distribution with mean of μ_{Y_z} and standard deviation of σ_{Y_z} , where μ_{Y_z} and σ_{Y_z} are, respectively, the mean and standard deviation of weekly meningitis cases in a simulated trajectory for which RNG seed z is used.

Component 4. Likelihood of periodicity in past meningitis epidemics

As described in a greater detail in §S8, to identify the significant periods at which past meningitis epidemics had occurred in Niger, we used the discrete Fourier transform. Let $\hat{\mathcal{F}}$ be the vector of Fourier amplitudes for the observed meningitis incidence time-series $\hat{Y} = (\hat{y}_1, \hat{y}_2, \dots, \hat{y}_T)$ (see §S8 for details on how $\hat{\mathcal{F}}$ can be calculated and Figure S12 for an example). Let \mathcal{F}_z be the vector of Fourier amplitude for the time-series $Y_z = (y_{z,1}, y_{z,2}, \dots, y_{z,T})$, the weekly meningitis cases during a simulated trajectory for which RNG seed z is used. We measure the likelihood of the observed $\hat{\mathcal{F}}$ given \mathcal{F}_z as the product of the likelihood of the angle between vectors $\hat{\mathcal{F}}$ and \mathcal{F}_z and the likelihood of the magnitude of vector $\hat{\mathcal{F}}$ (denoted by $\|\hat{\mathcal{F}}\|$) given \mathcal{F}_z :

1. The angle between vectors $\hat{\mathcal{F}}$ and \mathcal{F}_z is calculated as: $\hat{\theta}_z = \arccos(\frac{\mathcal{F}_z \hat{\mathcal{F}}}{\|\mathcal{F}_z\| \|\hat{\mathcal{F}}\|})$. Angle 0 implies a perfect match between the significant periods of two time-series, and hence we assume that $\hat{\theta}_z$ follows a truncated normal with minimum 0 and standard division $\sigma_{\hat{\theta}_z}$. We set $\hat{\theta}_z = 5.1$ which results in a truncated normal distribution with 95% of the distribution below 10 degrees.
2. The magnitude of vector $\hat{\mathcal{F}}$, i.e. $\|\hat{\mathcal{F}}\|$, is always a positive number and hence, we choose a normal distribution with mean $\|\mathcal{F}_z\|$ and standard deviation of $0.1\|\mathcal{F}_z\|$, truncated to be bounded from below at 0, to represent the likelihood of $\|\hat{\mathcal{F}}\|$ given \mathcal{F}_z .

Total pseudolikelihood

To summarize, we calculate the natural logarithm of the likelihood of observations given a simulated trajectory as:

$$\ln \mathcal{L}(\hat{\mathbf{T}}; \mathbf{T}_z) + \frac{1}{5} \sum_{k=1}^5 \ln \mathcal{L}(\hat{s}_i; \hat{S}_i, \rho_{z,i}) + \ln \mathcal{L}(\mu_{\hat{\mathcal{F}}}; \mu_{Y_z}, \sigma_{Y_z}) + \ln \mathcal{L}(\hat{\mathcal{F}}; \mathcal{F}_z), \quad (1)$$

where $\mathcal{L}(\hat{\mathbf{T}}; \mathbf{T}_z)$ is the pseudolikelihood of age-distribution of cases (Component 1 as explained above), $\mathcal{L}(\hat{s}_i; \hat{S}_i, \rho_{z,i})$ is the pseudolikelihood of carriage prevalence in age group i (Component 2), $\mathcal{L}(\mu_{\hat{\mathcal{F}}}; \mu_{Y_z}, \sigma_{Y_z})$ is the pseudolikelihood of average weekly incidence (Component 3), and $\mathcal{L}(\hat{\mathcal{F}}; \mathcal{F}_z)$ is the pseudolikelihood of periodicity of epidemics (Component 4).

We note that Eq. (1) provides an approximation to the true likelihood function which could not be calculated for our model due to the sparsity of data and unobservable compartments. Also, Eq. (1) assumes that the four components of the pseudolikelihood function are independent, and assumption that is necessitated by lack of data to characterize the correlation between these four components (for example, while a non-zero correlation between incidence and carriage time-series is expected, time-series data needed to estimate this correlation are not available).

Model Projections

The calibration period spans from 2002 to mid-2015 (13.5 years, see Figure 2). However, PMC vaccine induces longer-term immunity, and hence a full evaluation of the performance of vaccination strategies requires us to run the model beyond the calibration period. For this extended period, we assume that all model parameters determined through calibration remain the same beyond 2016, except for the external force of infection (represented by $s_{1,q}$), which repeats every 14 years (Table S6).

Table S3: Prior distributions of natural history parameters.

Parameter	Distribution/Value	Lower Bound	Upper Bound	Sources
Time until losing carriage in Carrier state*	Uniform	1 week	27 weeks	[76]
Time until losing immunity from carriage in Immune state*	Uniform	4 weeks	260 weeks	[77-79]
Ratio of time until losing immunity from disease to time until losing immunity from carriage (in Immune state)*	Uniform	1	20	[41, 77, 79]
Rate of progression a_i to invasive disease for age group <1 y	Uniform	0	0.00075	Experiments with the model and [33]
Ratio of rate of progression to invasive disease with respect to age group <1 y				Experiments with the model and [33]
Age group 1-4 y	Uniform	1.35	1.65	
Age group 5-14 y	Uniform	1.35	1.65	
Age group 15-29 y	Uniform	0.675	0.825	
Age groups 30-100+ y	Uniform	0.225	0.275	
Duration of disease**	1 week	-	-	[29]
Disease-associated mortality κ^{**}	10%	-	-	[80]

Parameters marked with * are sampled for each individual in a simulation. All other parameters are sampled once per simulation.

Parameters marked with ** use fixed values as mentioned in the 2nd column.

Table S4: Prior distributions of transmission parameters.

Parameter	Distribution/Value	Lower Bound	Upper Bound	Sources
Transmission parameter for age group <1 y*	1	-	-	Experiments with the model and [33]
Relative force of infection with respect to age group <1 y				Experiments with the model and [33]
Age group 1-4 y	Uniform	0.08	0.12	
Age group 5-14 y	Uniform	0.175	0.225	
Age group 15-29 y	Uniform	0.025	0.035	
Age groups 30-100+ y	Uniform	0.025	0.035	
Distance parameter φ^*	Uniform	0.03	0.03001	Experiments with the model and [33]

Parameters marked with * use fixed values as mentioned in the 2nd column.

All parameters are sampled once per simulation.

Table S5: Prior distributions of population structure on the first simulation year (% of population in states).

Parameter	Distribution	Lower Bound	Upper Bound	Sources
Carrier state	Uniform	0.01	0.12	Experiments with the model and [33]
Immune state	Uniform	0.01	0.85	Experiments with the model and [33]

All parameters use fixed values as mentioned in the 2nd column, and are sampled once per simulation.

Table S6: Prior distributions of seasonality parameters.

Parameter	Distribution	Lower Bound	Upper Bound	Sources
External annual variation $s_{1,q}$ for year $q \in [1,2,3, \dots 14]$	Uniform	0	0.75	Experiments with the model and [33]
Phase parameter s_2^*	-0.25	-	-	Experiments with the model and [33]

Parameters marked with * use fixed values as mentioned in the 2nd column.
All parameters are sampled once per simulation.

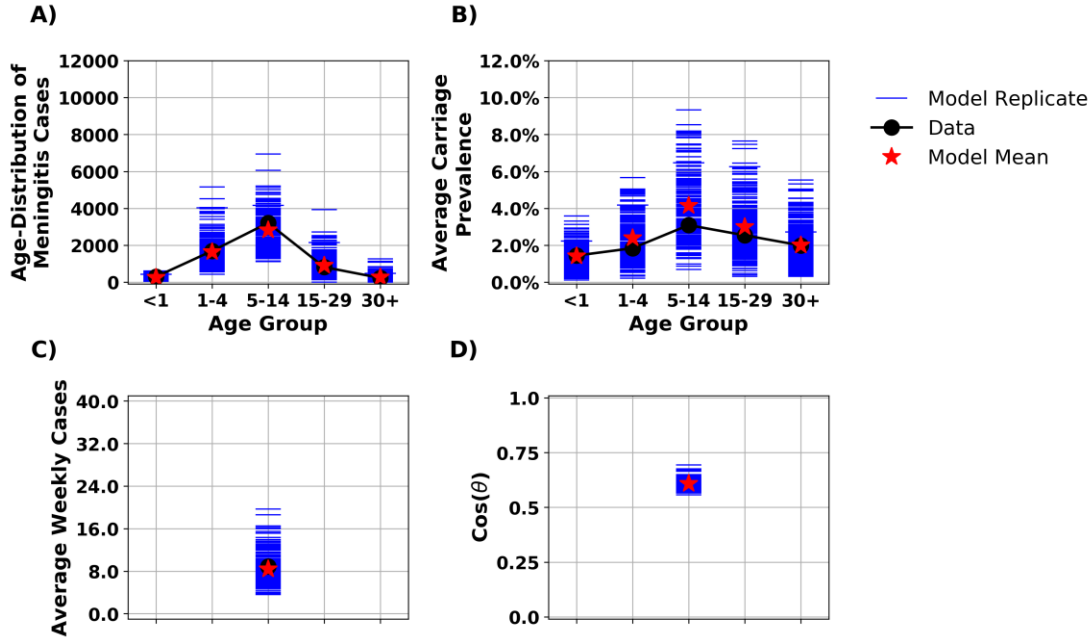


Figure S8: The proposed model matches the key characteristics of meningococcal epidemics in Niger between 2002 to mid-2015 for the no strain replacement scenario. A) Age-distribution of meningococcal meningitis cases in Niger versus the age-distribution of cases generated by the model. B) Estimated meningococcal carriage prevalence in different age groups from carriage survey studies in the African meningitis belt [19] versus the age-specific average carriage prevalence obtained from the model. C) Average of confirmed weekly meningococcal cases observed from 2002 to mid-2015 versus those produced by the model. D) Cosine of the angle (θ) between the vectors of Fourier amplitude for observed and simulated meningitis time-series; cosine of 1 indicates total match in periodicity and cosine of 0 indicates no overlap between the significant periods of two time-series.

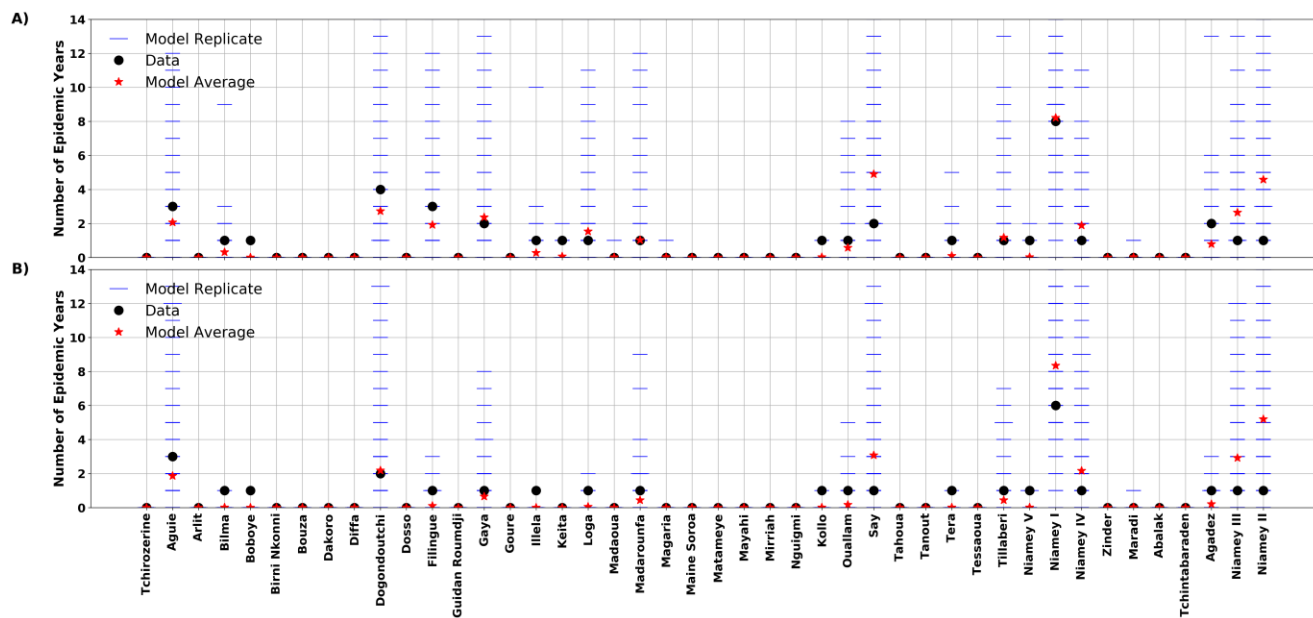


Figure S9: Number of years between 2002 to mid-2015 when the weekly meningitis clinical cases pass the WHO epidemic threshold in Niger's districts produced by our model and observed in the data for the no strain replacement scenario. A) Complete strain replacement scenario. B) No strain replacement scenario.

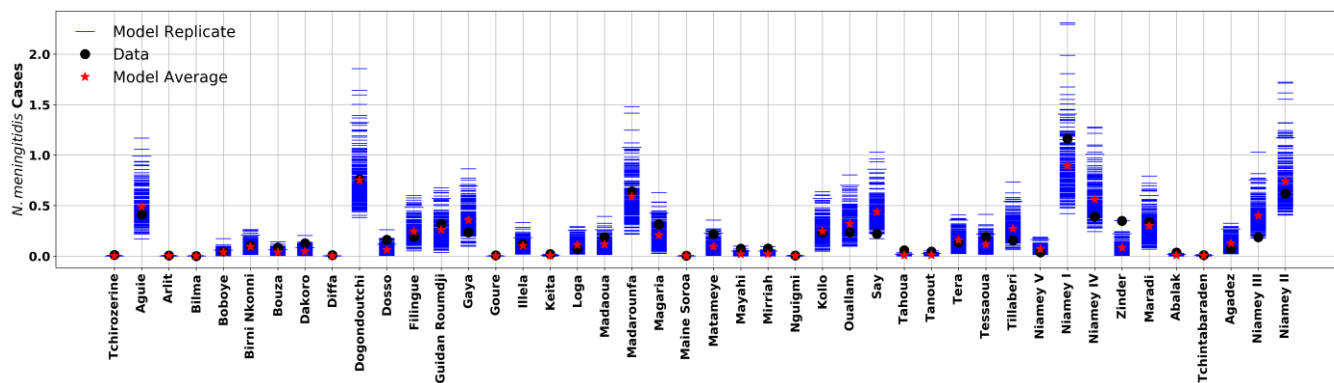


Figure S10: Average weekly *N. meningitidis* cases in Niger's districts produced by our model and observed in the data for the no strain replacement scenario.

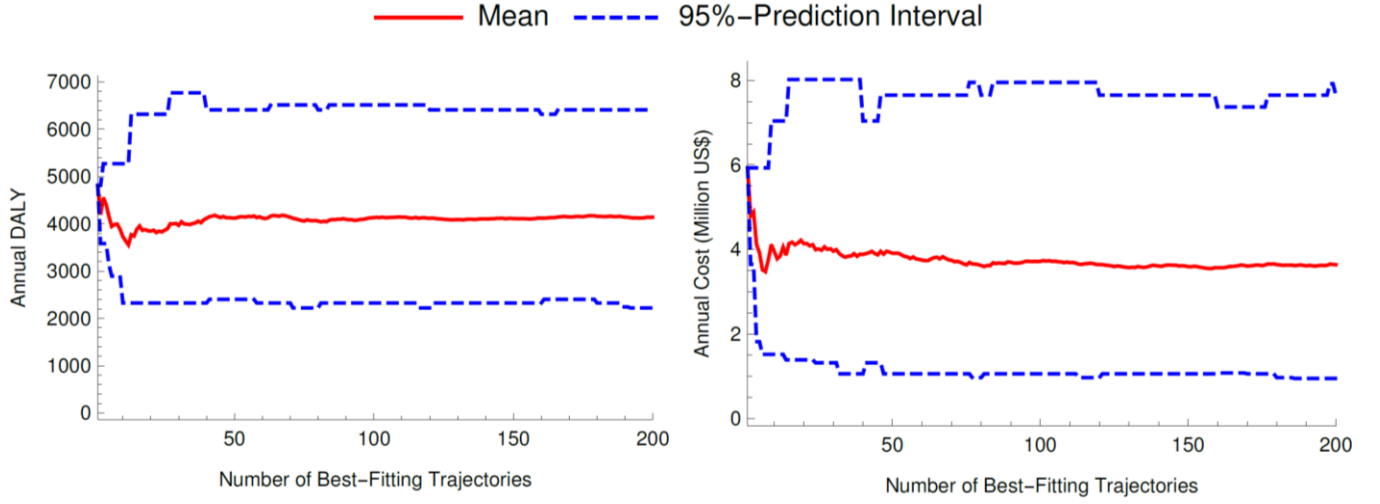


Figure S11: The mean and 95% prediction interval of the estimated annual DALY and cost for the strain-replacement scenario under the Base strategy. In these figures, means and prediction intervals are calculated using the n best-fitting trajectories among $500n$ trajectories each of which uses parameter values that are randomly drawn from the prior probability distributions listed in Table S3-Table S5. This figure suggests that calibrating the model using more than 100,000 simulated trajectories is not expected improve the accuracy of estimated means and prediction intervals.

S8 Characterizing Periodicity of Past Epidemics

We use the Discrete Fourier transform (DFT) of weekly meningitis cases in Niger over 2002-2016 to identify the significant periods of past meningitis epidemics [33]. The Discrete Fourier transform of time-series $(f_0, f_1, \dots, f_n, \dots, f_{N-1})$ is defined as:

$$F_k = \sum_{n=0}^{N-1} f_n e^{-2\pi i k n / N}, k \in \{0, 1, \dots, N-1\},$$

where $e^{-2\pi i k n / N} = \cos\left(2\pi k \frac{n}{N}\right) - i \sin\left(2\pi k \frac{n}{N}\right)$, $k \in \{0, 1, \dots, N-1\}$, represent N Fourier bases with corresponding periods $\frac{N}{k} dt$ where dt is the time between two adjacent points in the time-series (in our case, 1 week), and F_k represents projection of the time-series $(f_0, f_1, \dots, f_n, \dots, f_{N-1})$ onto the corresponding Fourier bases. Since the meningitis incidence time-series is real-valued, $F_k, k \in [0, 1, \dots, \lfloor \frac{N}{2} \rfloor]$ represents all the periodicity of the signal with F_0 representing zero frequency (or simply the sum of the time-series) and $F_{\lfloor N/2 \rfloor}$ representing maximum possible frequency (Note: $\lfloor N/2 \rfloor = N/2$ if N is an even number and $\lfloor N/2 \rfloor = (N-1)/2$ if N is an odd number). For a comprehensive review of Fourier transform, refer to the tutorial by Duhamel and Vetterli [81]. $|F_k|^2$ is referred to as Fourier amplitude and we use $F = (|F_0|^2, |F_1|^2, \dots, |F_{\lfloor N/2 \rfloor}|^2)$ to denote the vector of Fourier amplitudes.

To identify significant periods of a time-series (i.e. periods for which $|F_k|^2$ is statistically greater than zero), we generate 1,000 bootstrap resamples of the time-series by randomly shuffling the time-points of the original time-

series [82]. This process removes the inherited periodicity in each resampled time-series. We next use DFT to calculate the Fourier weights $|F_k|^2$, $k \in [0, 1, \dots, N - 1]$, for each bootstrap resampled time-series. We consider the period that corresponds to the Fourier weight $|F_k|^2$ statistically significant, if $|F_k|^2$ calculated for the original time-series is greater than 99% of the $|F_k|^2$ calculated from the 1,000 bootstrap samples. Figure S12 displays the significant periods of weekly meningitis cases in Niger between 2002-2016 identified using the approach described above.

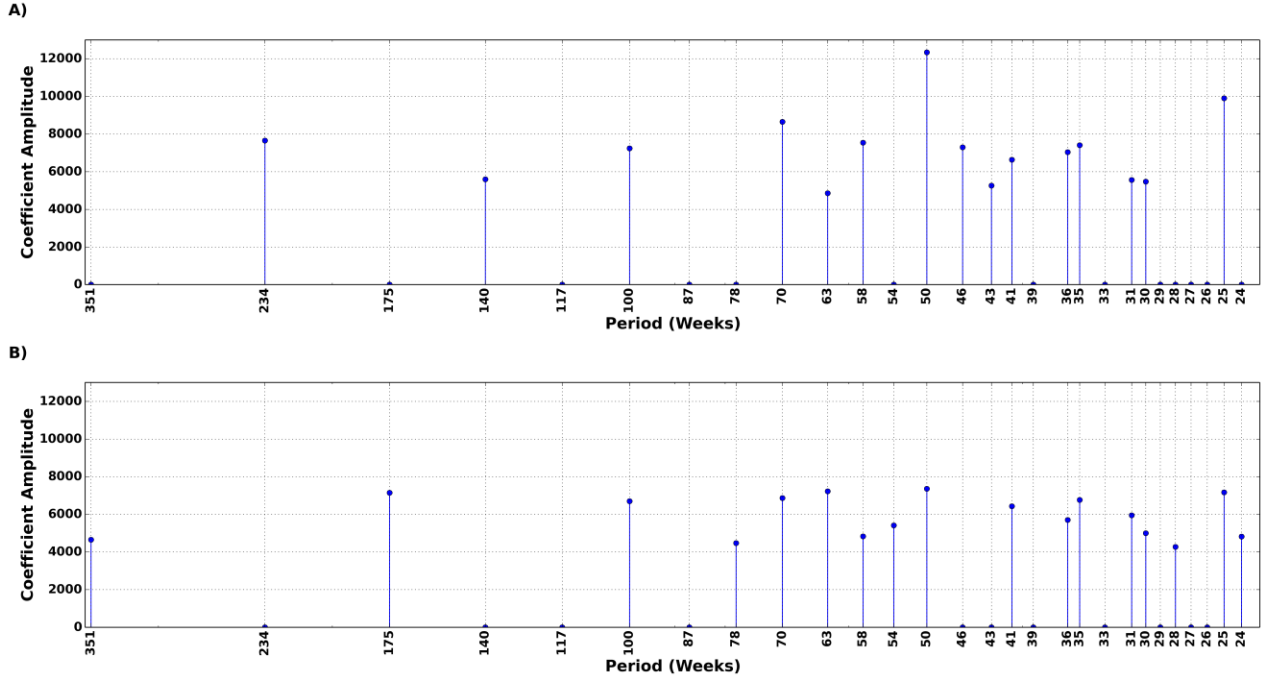


Figure S12: Significant periods of weekly meningitis cases observed in Niger reported between 2002 to mid-2015 as displayed in Figure 2. A) Complete strain replacement scenario. B) No strain replacement scenario.

As part of calibration, we also compared the age structure of the population of Niger [66] with that from sample simulations (example illustrated in Figure S13).

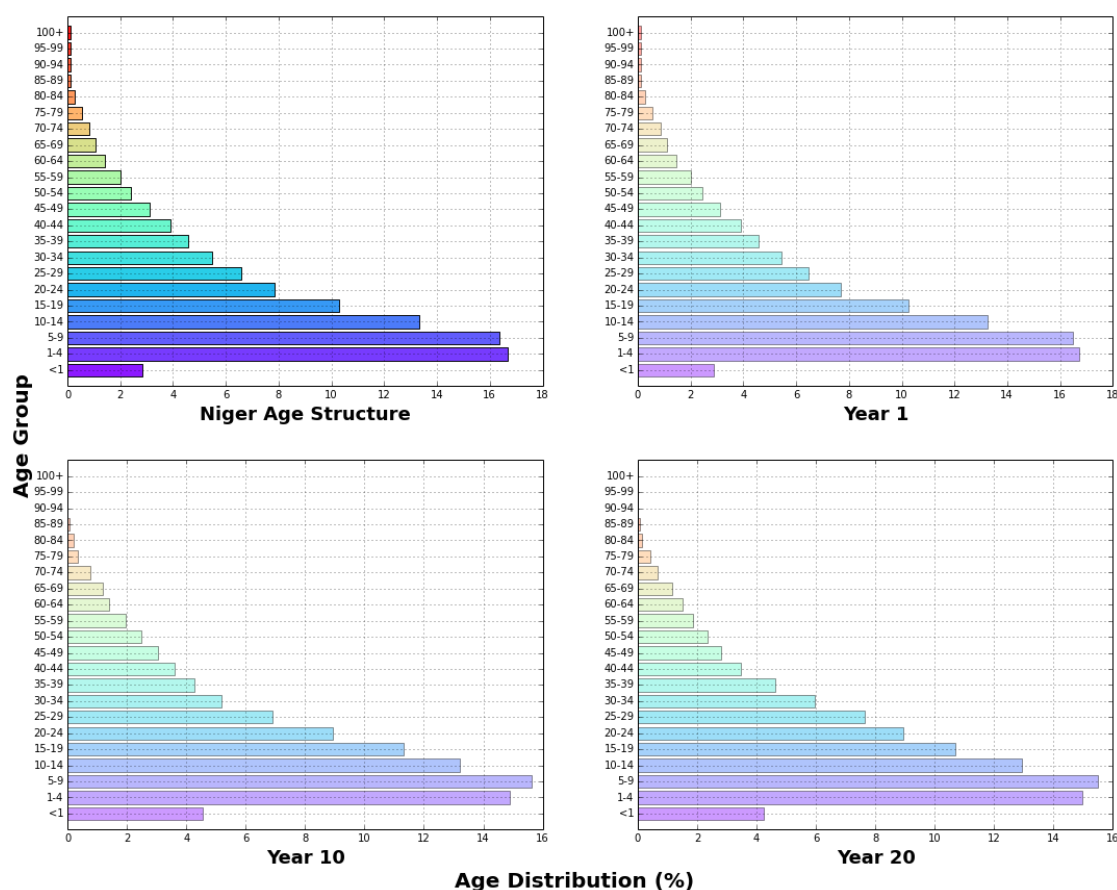


Figure S13: Comparing the 2016 age structure of Niger (A) with that produced by the simulation model in years 1 (B), 10 (C) and 20 (D).

S9 Cost and DALY Calculation

We use disability-adjusted life-years (DALY) to measure the health outcomes associated with alternative vaccination strategies. To measure the financial outcomes, we consider disease-related costs (such as case management cost and care cost for sequelae-experiencing patients) and vaccine costs of vaccination campaigns. The summary of cost parameters is provided in Table S7. All health and financial outcomes of alternative vaccination strategies are discounted at an annual rate of 3% to 2016. All costs are presented in the US dollars.

In the absence of reliable cost data related to meningitis case management in Niger, we use US \$50.73 (estimated in 2015 from a cost study in Burkina Faso [83]; \$51.74 in 2016) as an estimate for the costs of meningitis case management. This estimate includes direct medical costs (e.g. drugs, consultations, laboratory analyses for case diagnosis), direct non-medical costs (e.g. transportation and food), and other indirect costs [33, 84]. In Burkina Faso, on average, 7.2% of those surviving a meningitis episode will experience major sequelae, and the concerned

household incur an additional cost of US \$25.4-\$154.4 for rehabilitation [84]; hence, we assume that short-term cost of sequelae follows a Uniform distribution of [\$25.4-\$154.4].

We use vaccine delivery cost of \$0.28 (estimated in 2010, \$0.31 in 2016) per dose for routine vaccination programs that include service delivery, advocacy and communication, monitoring and disease surveillance, program management [83]. To calculate the total vaccine doses required for routine immunization, we assumed a wastage factor of 1.67 [83]. For both reactive and preventive vaccination campaigns, we assume that the vaccine delivery cost (which includes transportation, advocacy and communication, personnel, monitoring and disease surveillance, cold chain equipment, and program management) is US \$0.43 (estimated in 2007, \$0.51 in 2016) per person [85].

Vaccine and injection supplies are major contributors to recurring costs during reactive and preventive campaigns [85]. We assume \$0.15 for injection supplies [86]. For vaccine costs, we assume \$0.64 and \$4 for *MenAfriVac*TM and PMP vaccine (per dose), respectively [87]. Since the PMC vaccine price is not yet determined, we vary this price from \$4 to \$10 per dose.

Table S7: Cost parameters.

Parameter	Cost	Sources
Meningitis case management	\$51.74	[83]
Meningitis sequelae	Uniform [\$25.4 – \$154.4]	[84]
<i>MenAfriVac</i> TM vaccine	\$0.64 per dose	[87]
PMP vaccine	\$4 per dose	[87]
PMC vaccine	\$4 – \$10 per dose	Price is not determined yet; varied between \$4.0 and \$10.0 in a sensitivity analysis [33]
Injection supply	\$0.15 per vaccinated person	[86]
Vaccine delivery costs		
Routine programs	\$0.52 per vaccinated person	The delivery cost is estimated \$0.31 per dose for routine vaccination programs [83] and we used a wastage factor of 1.67 [83] to estimate delivery cost per vaccinated person ($\$0.31 \times 1.67 = \0.52).
Reactive campaigns	\$0.51 per vaccinated person	[85]
Preventive campaigns	\$0.51 per vaccinated person	[85]

S10 Sensitivity Analysis: Impact of PMC Vaccine Price on the Performance of Vaccination Strategies

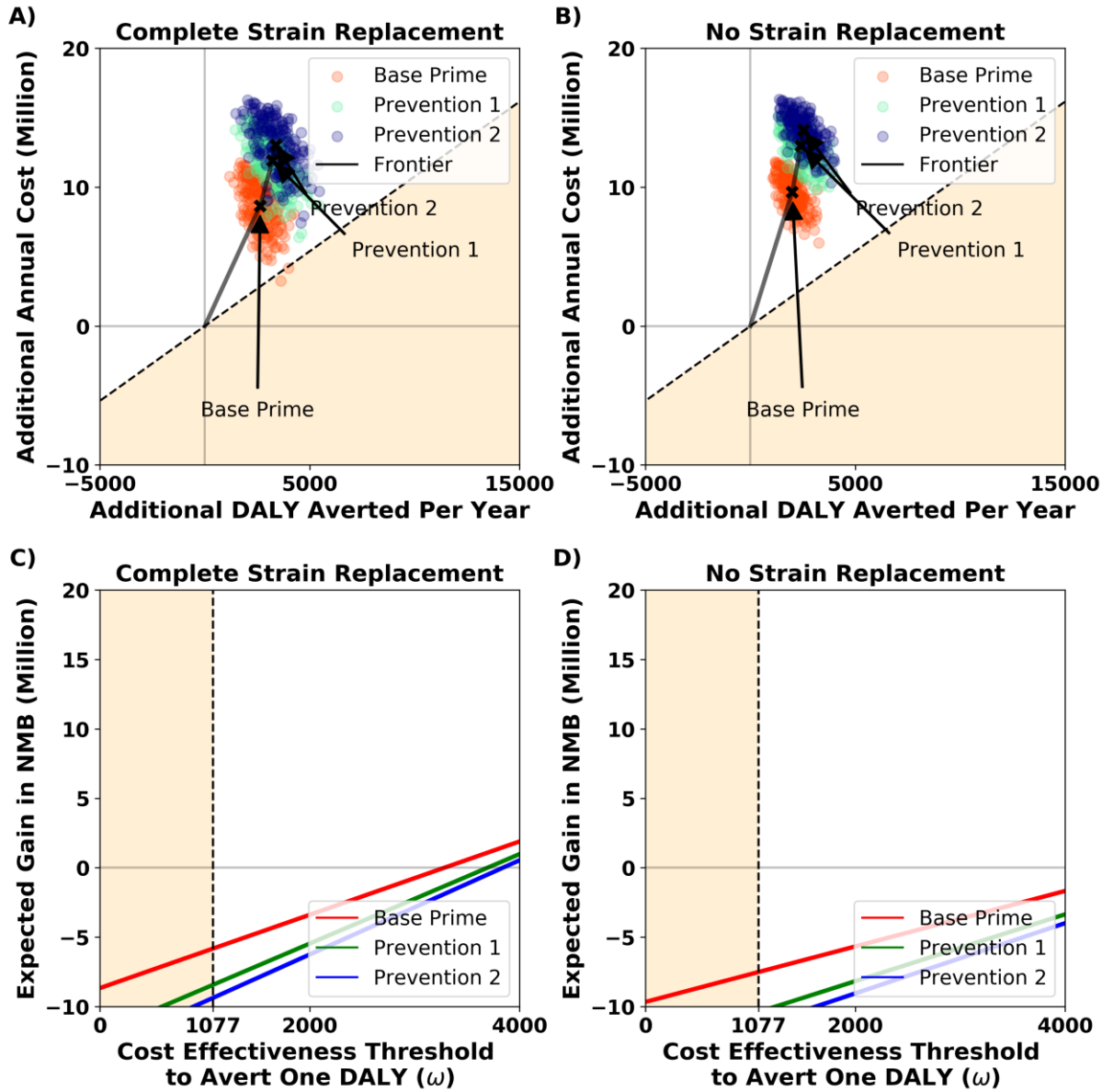


Figure S14: Economic evaluation of vaccination strategies described in Table 3 for the complete strain replacement scenario (A, C) and the no strain replacement scenario (B, D). The price of PMP and PMC vaccines are \$4 and \$10 per dose, respectively. In figures C and D, the expected gain in net monetary benefit (NMB) of a strategy is calculated with respect to the Base strategy. The dashed line in these figures represents the cost-effectiveness threshold of three per capita gross domestic product of Niger which is estimated to be 3×359 USD in 2015 [45]. All costs and DALYs are discounted at rate 3% to year 2016.